

Supporting Information

Porrello et al. 10.1073/pnas.1208863110

SI Methods

Experimental Animals. All protocols were approved by the Institutional Animal Care and Use Committee of the University of Texas Southwestern Medical Center. Timed-pregnant ICR/CD-1 mice (Charles River Laboratories) were used to deliver pups for neonatal surgical procedures.

TTC Staining. To distinguish among infarcted area, area at risk, and unaffected remote myocardium after ischemia/reperfusion (I/R) injury, a water-soluble dye (Evans blue) was injected to stain the remote myocardium followed by TTC staining. The percentage of infarcted (white), area at risk (red), and unaffected remote (blue) myocardium 24 h after I/R was quantified by using Image J software (National Institutes of Health), as described (1).

Vascular Corrosion Casting. To visualize the coronary anatomy of the neonatal mouse heart after left anterior descending (LAD) ligation, coronary vascular casts were prepared at 7 and 21 d after myocardial infarction (MI). Mice were anesthetized and hearts were dissected out before being placed in PBS containing heparin. The casting compounds (Polysciences; Batson's number 17; 5-mL monomer base, 1.5-mL catalyst, 0.1-mL promoter) were mixed and retrogradely perfused into the aorta through a cannula placed above the aortic valve. The cast was left to set for 3 h at room temperature, followed by overnight incubation at 37 °C in saturated potassium hydroxide solution to dissolve the surrounding tissue.

Immunofluorescence. For BrdU/PECAM-1 costaining, cryosections were fixed for 10 min in ice-cold acetone. Slides were rinsed with 0.1% (vol/vol) Triton X-100 in PBS twice for 5 min and blocked in 5% goat serum for 30 min. Slides were incubated with an unconjugated primary antibody against PECAM-1 (1:20, rat monoclonal; BD Biosciences) overnight at 4 °C. Slides were washed three times in PBS and incubated with goat anti-rat secondary antibody conjugated to Alexa Fluor 488 (1:400; Invitrogen) for 1 h at room temperature. For BrdU costaining, a BrdU staining kit was used (catalog no. 93-3943; Invitrogen). Slides were permeabilized

with denaturing solution for 30 min. Slides were rinsed three times with PBS followed by incubation with the blocking solution for 30 min. Slides were incubated with a biotinylated BrdU antibody for 1 h at room temperature. Slides were washed three times in PBS and incubated with a streptavidin secondary antibody conjugated to Alexa Fluor 555 (1:200; Invitrogen) for 1 h at room temperature. Slides were washed three times in PBS and mounted in Vectashield containing DAPI (Vector Laboratories).

Cardiac Troponin-I Measurements. To document myocardial necrosis in anti-miR- and mismatch-treated mice after ischemia-reperfusion (I/R), serum was collected at 24 h after I/R. Serum cardiac troponin levels were measured by using a high-sensitivity mouse cardiac troponin-I (cTnI) ELISA kit, according to the manufacturer's instructions (Life Diagnostics).

Microarray Analysis. Microarray analysis was performed on RNA samples extracted from cardiac ventricles (below ligature) from β MHC-miR-195 transgenic and wild-type mice 7 d after MI at postnatal day (P)1. Microarray analysis was performed by the University of Texas Southwestern Microarray Core Facility by using the Mouse WG-6 v2.0 Array (Illumina) as described (2).

Gene Ontology Cluster Analysis. Gene ontology analysis was performed for genes that were significantly regulated in miR-195 TG vs. WT hearts at 7 d after MI at P1 (>1.2-fold). Gene ontology analysis was conducted by using the Database for Annotation, Visualization, and Integrated Discovery (DAVID) functional annotation tool. DAVID analysis was performed with "Medium" classification stringency and *P* value cutoff of 0.01.

Statistical Analysis. All data are presented as mean \pm SEM. Student's unpaired *t* test was used for comparisons between two groups. A paired *t* test was used for comparisons between two groups where repeated measures were obtained in individual mice at different time points (e.g., echocardiographic data recorded at multiple time points after MI). A value of *P* < 0.05 was considered significant.

1. Bohl S, et al. (2009) Refined approach for quantification of in vivo ischemia-reperfusion injury in the mouse heart. *Am J Physiol Heart Circ Physiol* 297(6):H2054–H2058.

2. Davis CA, et al. (2006) PRISM/PRDM6, a transcriptional repressor that promotes the proliferative gene program in smooth muscle cells. *Mol Cell Biol* 26(7):2626–2636.

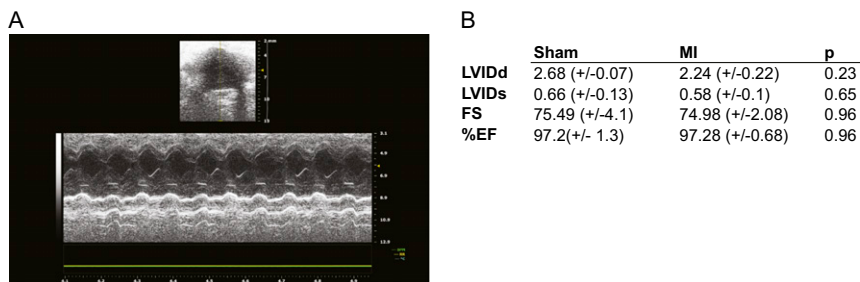


Fig. S1. Left ventricle (LV) function 9 mo after MI at P1. (A) M-mode echocardiography 9 mo after MI at P1 showing normal LV systolic function. (B) Left ventricular internal diameter at end diastole (LVIDd) and end systole (LVIDs) were used for calculating fractional shortening (FS) and ejection fraction (EF). Values presented as means \pm SEM; *n* = 3 (sham) and *n* = 6 (MI).

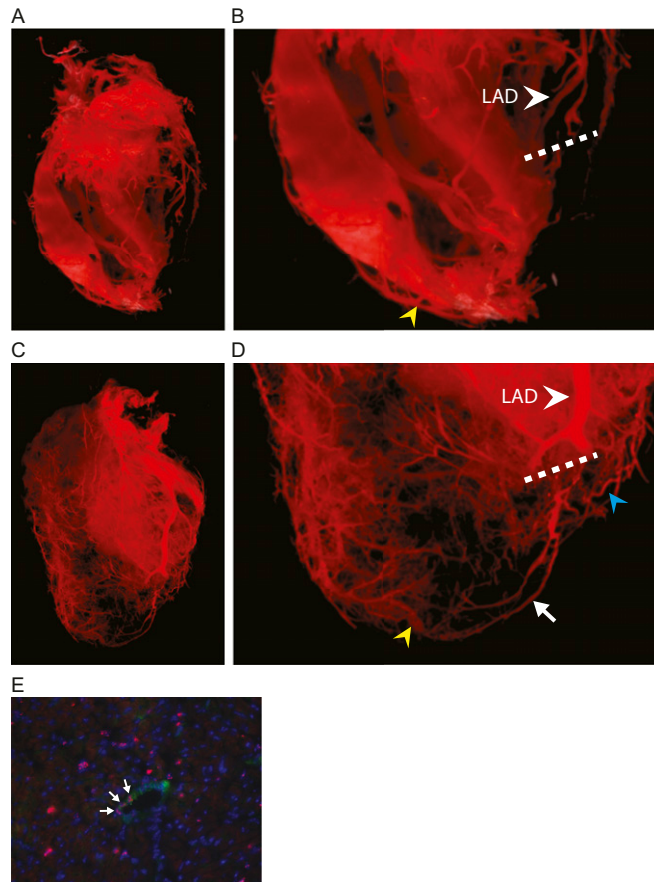


Fig. S2. Post-MI collateralization and neovascularization. (A and B) Low and high magnification images of coronary corrosion casts at day 7 after MI. (C and D) Low and high magnification images of coronary corrosion casts at day 21 after MI. White arrowhead indicates LAD, and dotted line indicates site of ligation. White arrow shows vascularization of the left ventricular anterior wall distal to the ligation. Right-to-left (yellow arrowhead) and left-to-left (blue arrowhead) collaterals are also shown. (E) Image showing BrdU (red) colocalization with PECAM (green) at day 21 after MI at P1. Arrows denote a BrdU⁺/PECAM⁺ blood vessel in the infarcted heart.

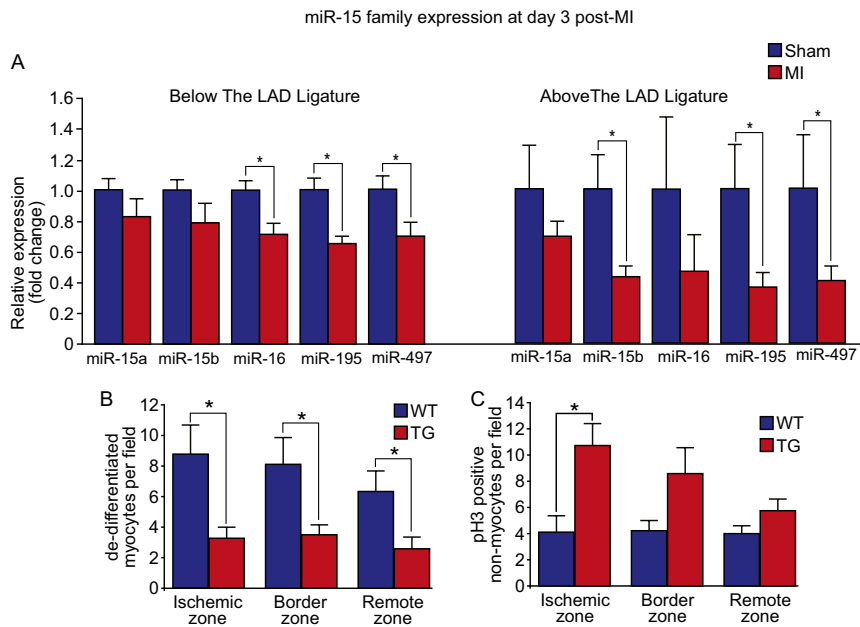


Fig. S3. miR-195 overexpression inhibits neonatal MI. (A) Real-time PCR analysis of miR-15 family (miR-15a, -15b, -16, -195, -497) expression levels at day 3 after MI at P1 from heart tissue taken below and above the ligature. miR expression levels are normalized to U6 and presented as a fold change relative to sham controls (dotted line at 1.0). Values presented as mean \pm SEM; $n = 4-5$ per group; $*P < 0.05$. (B) Quantification of the number of cardiomyocytes with disassembled sarcomeres in WT and TG mice at day 7 after MI. Quantitative analyses represent counting of multiple fields from three WT and four TG samples per group (~ 9 fields per region). Values presented as mean \pm SEM; $*P < 0.05$. (C) Quantification of the number of pH3⁺ nonmyocytes in WT and TG mice at day 7 after MI. Quantitative analyses represent counting of multiple fields from three WT and four TG samples per group (~ 9 fields per region). Values presented as mean \pm SEM; $*P < 0.05$.

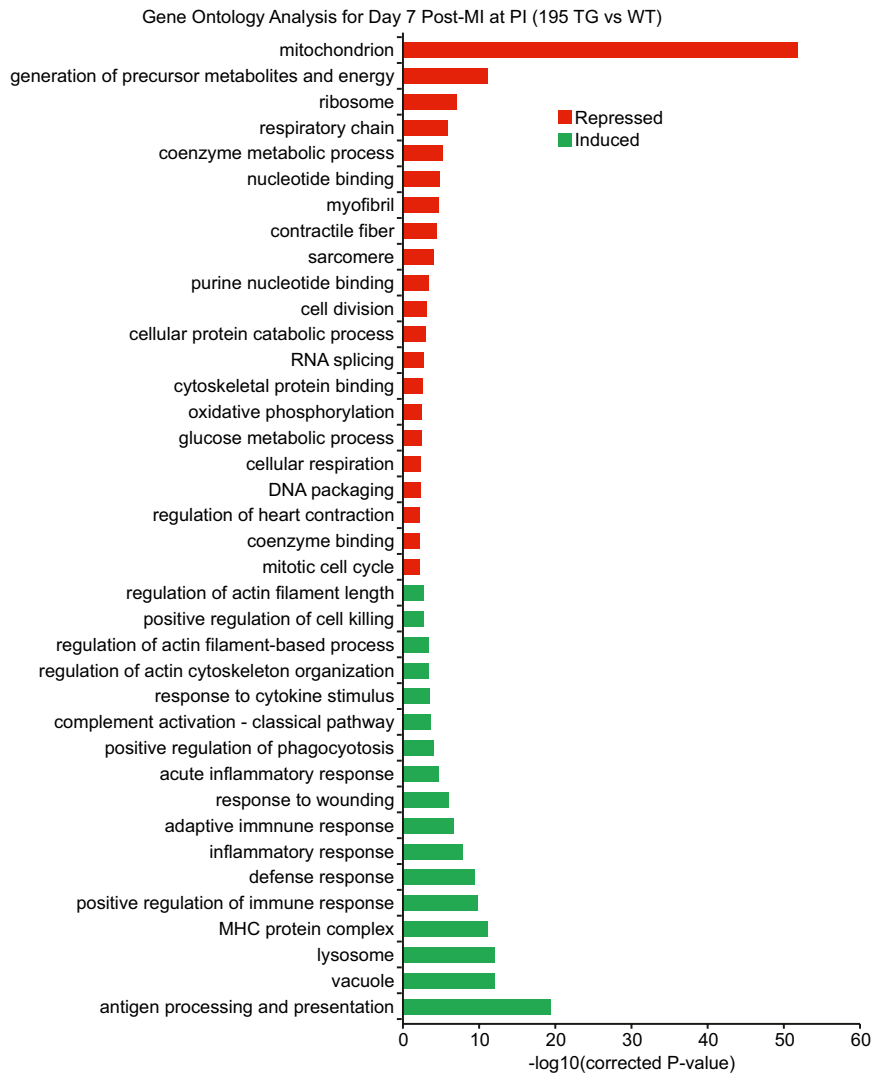


Fig. S4. Ontology analysis of genes differentially regulated in miR-195 transgenic hearts after MI at P1. Genes that were either repressed (red) or induced (green) in miR-195 TG vs. WT hearts at day 7 after MI at P1 were clustered on the basis of shared ontology by use of the DAVID algorithm. A corrected P value of <0.01 was considered significant.

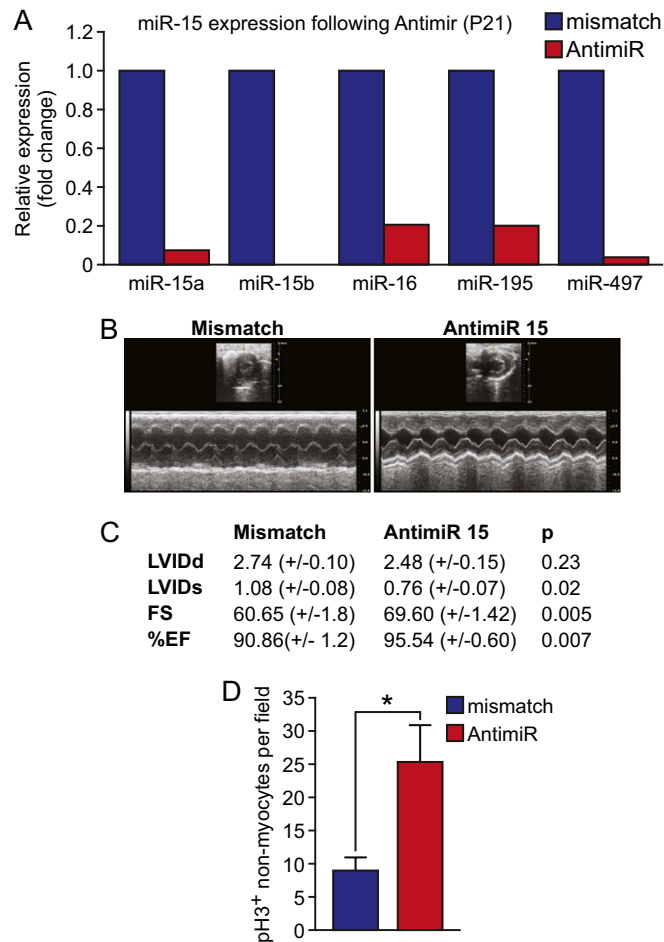


Fig. S5. Postnatal inhibition of the miR-15 family enhances cardiac function after I/R injury. (A) Real-time PCR analysis of miR-15 family member expression in the heart at postnatal day (P)21, after administration of miR-15b/16 anti-miRs at P1, P7, and P14. miR expression levels are normalized to U6 and presented as a fold change relative to mice treated with a mismatch control. (B) Representative images of M-mode echocardiogram showing enhanced cardiac function in anti-miR-15 treated mice compared with mice treated with a mismatch control. (C) Left ventricular internal diameter at end diastole (LVIDd) and end systole (LVIDs) were used for calculating fractional shortening (FS) and ejection fraction (EF). Values presented as means \pm SEM; $n = 4$ (mismatch) and $n = 5$ (anti-miR). (D) Quantification of the number of pH3⁺ nonmyocytes in anti-miR and mismatch treated mice at day 7 after I/R injury at P21. Quantitative analyses represent counting of multiple fields from five mismatch and four anti-miR samples per group (~ 9 fields per sample). Values presented as mean \pm SEM; * $P < 0.05$.